The Orbital Debris Quarterly News

January 2002 — Volume 7, Issue 1

NEWS

Two Major Satellite Breakups Near End of 2001

Two major satellite breakups, the worst in 20 months, occurred just four weeks apart in the fourth quarter of 2001, both producing in excess of 300 large fragments. Two other lesser breakup events brought the total number of satellite fragmentations to nine for the year, a rate not matched since 1998.

On 21 November a Russian satellite, Cosmos 2367 (International Designator 1999-072A, US Sat. No. 26040), experienced a significant fragmentation while in an orbit just 30 km above the International Space Station (ISS), i.e., 411 km mean altitude for Cosmos 2367 and 382 km for ISS. Approximately 200 debris were detected by normal US Space Surveillance Network (SSN) operations, while special sensor observations several days after the event indicated that another 100 or more smaller debris were also in orbit. These debris were concentrated in the orbital regime of 200-500 km, but some were thrown into orbits with apogees above 1000 km.

Approximately 40% of the debris were immediately thrown into orbits which crossed the orbit of ISS. Immediately upon notification of the breakup, the Orbital Debris Program Office undertook an effort to characterize the probable debris cloud and to assess the risks posed by it not only to the ISS but also to the imminent STS-108 mission. Naval Space Command, headquartered in Dahlgren, Virginia, spearheaded the effort to identify the individual debris and to develop initial orbital parameters

for each. Throughout Thanksgiving and the following weekend, NASA and Naval Space Command personnel worked to gain a better insight into the extent of the newly created debris cloud.

The STS-108 mission, then planned for launch on 29 November, raised new safety issues. The Space Shuttle is not as well protected from small debris impacts as ISS. Specific concerns were STS-108 overall mission risks, EVA risks, risks associated with boosting ISS during the mission, and risks associated with special Space Shuttle attitudes planned during independent flight. Fortunately, these new risks were assessed to be within NASA guidelines.

Cosmos 2367 was the latest in the Cosmos 699 series of 3-metric-ton spacecraft which began in 1974. To date 20 of these spacecraft have undergone one or more fragmentation episodes with the number of debris generated usually on the order of 100 or more. Most of the events have occurred at relatively low altitudes, resulting in relatively rapid decay of the debris. In the case of Cosmos 2367 some of the debris should remain in orbit for many months.

About three weeks after the Cosmos 2367 breakup, the 12-year-old Molniya 3-35 spacecraft (International Designator 1989-043A, US Sat. No. 20052) fragmented during catastrophic orbital decay on 14 December while passing over the Southern Hemisphere. About two dozen pieces were detected with most reentering immediately. Some debris appear to have

remained in orbit for a few more revolutions before falling back to Earth.

On 19 December the eighth breakup of the year resulted in a severe fragmentation of an Indian PSLV fourth stage (2001-049D, US Sat. No. 26960), which had been in orbit for only two months. Within two days of the event approximately 200 debris with orbits stretching from 200 to 1100 km had been identified. By 27 December the number of tracked debris surpassed 300. The event marked the first breakup of an Indian satellite.

This was the sixth flight of the PSLV (Polar Satellite Launch Vehicle) which had successfully inserted the main payload, the Indian TES (Technology Experiment Satellite) spacecraft, into a sun-synchronous orbit along with a small German satellite called BIRD. A second piggyback satellite from Belgium, PROBA, was placed into a slightly elliptical orbit after the deployment of TES and BIRD. The 900 kg stage was in an orbit of 550 km by 675 km with an inclination of 97.9 deg at the time of the event.

The cause of the PSLV breakup is under investigation. A potential energy source for the fragmentation may be residual hypergolic propellants. The release of all residual propellants and compressed fluids at the end of launch vehicle stage and spacecraft operations is highly recommended by US Government agencies as well as many space-faring nations around the

Inside...

NEWS

Two Major Satellite Breakups Near End of 2001, Cont'd

(Continued from page 1)
world. To date no satellite which has been successfully passivated in this manner is known to have suffered a breakup.

The final fragmentation of the year appears to have occurred late on 24 December when a 10-year-old Ariane 4 orbital stage generated several pieces of debris. The stage (1991-075B, US Sat. No. 21766) had placed the Intelsat 601 spacecraft into a geosynchronous transfer orbit on 29 October 1991. The orbit of the stage at the time of the event was 230 km by 28,505 km with an inclination of 7.2 deg. The extent of the fragmentation was still being evaluated at the close of 2001. ❖

Anomalous Events in 2001

Anomalous events are defined as the unplanned separation, usually at low velocity, of one or more detectable objects from a satellite which remains essentially intact. The principal causes of anomalous events are assessed to be impacts by very small natural or artificial particles or to be the result of environmental stresses leading to satellite surface degradations. Anomalous events are historically more difficult to identify than the more intense and prolific satellite breakups. The latest edition of "History of On-Orbit Satellite Fragmentations" (JSC-29517, July 2001) lists 35 satellites which have suffered one or more anomalous events.

The 1st Command and Control Squadron (1CACS) of Air Force Space Command has found evidence for anomalous events with at least three satellites during 2001. Each event produced a single new piece of debris. The first event occurred early in the year, perhaps in April, when an object separated from the Ariane 40 launch vehicle (1991-050F, US Sat. No. 21610) which had launched the ERS-1 spacecraft. The object, eventually cataloged as US Sat. No. 26925, experienced considerably higher orbital decay than its parent, which was in a nearly circular orbit with a mean altitude of about 770 km. Reentry is expected to occur in 2002.

The second anomalous event involved the 35-year-old Nimbus 2 spacecraft (1966-040A, US Sat. No. 02173), which has been the subject of multiple anomalous events since 1997. The newly detected event is assessed to have occurred about the start of May 2001. A single object was released and later cataloged as US Sat. No. 26962. This object also is decaying more rapidly than Nimbus 2 from its original 1093 km by 1177 km orbit.

Seasat (1978-064A, US Sat. No. 10967), which also has been linked to several anomalous events since 1983, was the third source of new debris identified by analysts of 1CACS. The new fragment (US Sat. No. 26963) appeared in early July with a very high rate of decay, falling from an altitude of more than 750 km to reentry in only five months. Many of the previous Seasat anomalous event debris also exhibited high area-to-mass ratios which resulted in rapid orbital decay.

The orbital lifetimes of two of these three debris were sufficiently short, thereby posing no long-term collision risk to other resident space objects. This is typical of a large number of anomalous debris and is a clue to their character. The Orbital Debris Program Office will be releasing the results of a new study on anomalous events and their potential importance next year. ❖

The 2001 Leonid Observations at JSC

J. Pawlowski

The JSC Leonid Observers were out and about in the wee hours of Sunday morning, November 18, 2001.

Mark Mulrooney and Anna Scott observed at the JSC Observatory near Cloudcroft, New Mexico. Observing about 1/6th of the sky, Anna counted a peak of 700 between 1000 and 1100 UT. Mark wrote, "Having viewed showers for 25 years, I've never seen anything like it". Mark estimated a ZHR of 1000 to 2000 from 1000-1200 UT. He also noted that many of the meteors appeared green with golden tails. " A few bolides showed up during the peak on November 18th. Very subjectively I would say there were proportionally more bolides the night after the peak although the rate was substantially diminished." Additionally, these astronomers recorded this event using our Liquid Mirror Telescope (LMT). This video data will be analyzed and be available to the public in the next few months.

Gene Stansbery observed from his hammock in Friendswood Texas near his backyard landing strip. "The show was very good even from suburban Houston. I layed out in my ham-mock in my back yard starting about 3:30. I did have to deal with the runway lights which ended up being brighter than I would have imagined. I saw a meteor about once every 10 seconds for the first hour or so. After that, sleep and fog took their toll and the rate dropped considerably by 5:00 a.m."

Jim Pawlowski was not as fortunate. He was visiting his daughter, Amber, in La Jolla California and observed a few Leonids on the side of a country road east of El Cajon. Cloudy skies limited his success.

Jim's friend, George Varros, had amazing luck at his observation location, Mount Airey, Maryland. Some of his video can be found at www.space.com whereas his complete collection is found at www.gvarros.com.

Paul Maley observed from a site near meteor Crater, Arizona. He reports, "I have 101 Leonids on video plus 93 train remnants." He also got a magnitude −10 head echo on his video.

Mark Matney was strategically placed in North Texas, where he was clouded out for 100 miles in every direction.

Pat Jones, observing from his back yard in Clear Lake, Texas, considers this the greatest meteor shower he's ever seen. "In a one-hour period I observed eight meteors. From Houston, that's the best I've ever seen. It was almost worth getting up at that ungodly hour to see it!"

Kandy Jarvis reported, "The view of the Leonids from Las Vegas (~45 min drive North of downtown) wasn't bad, though a brisk wind made it a bit teeth chattering. Humidity was high and there was significant scintillation and a wispy, ethereal light fog. (Unfortunately a temperature inversion was occurring at this time in Las Vegas.) Leonids were viewed from about 2 am to 3 am and at its peak. Though only half the sky was visible due to the house and huddling in blankets, meteors were viewed at about 1 every 4 seconds. No large brilliant balls were observed, but many faint sparklers and some nice strong but short ones were seen. Starting around 2 am, meteors were seen at a rate of a few every minute increasing to 1 every 10 count, to its peak of 1 every second or so. The cold chased this observer in at about 2:50 am local Las Vegas time." ❖

NEWS

Hypervelocity Impact Testing Of Betacloth Covers On Space Shuttle Orbiter Radiator External Lines

F. Lyons and E. Christiansen

Hypervelocity impact (HVI) tests were conducted by the NASA JSC Hypervelocity Impact Technology Facility (HITF) to evaluate meteoroid and orbital debris (M/OD) impacts to the Shuttle radiator interconnect lines (0.035" thick Aluminum alloy 5083-H32) protected by either one or two-layers of beta-cloth. An objective of the test program was to determine projectile sizes that will fail the Shuttle radiator lines for the two protection configurations (one and two-layers of beta-cloth) as a function of impact velocity and angle. Failure criteria is defined as a complete perforation (through-crack or hole) of the line (not pressure tight). Another objective was to determine impact conditions that result in damage similar to impact damage observed during Shuttle post-flight inspections. Results from thirty-five HVI tests are documented in report (JSC-28524).

This work was initiated due to the two significant craters found on OV-104 (*Atlantis*) external radiator interconnect lines after STS-86 (JSC-28033). Post-flight surveys of meteoroid/orbital debris impacts on the Space Shuttle Orbiter are conducted to identify damage caused by hypervelocity impacts and to identify the source (i.e., whether meteoroid or orbital debris) of the projectiles responsible. As illustrated in Figure 1, one of the impacts left a 0.8 mm diameter by 0.47 mm deep crater in the external line while another impact crater measured 1.0 mm diameter by 0.36 mm deep. Analysis of samples taken from the first impact indicated the presence of iron, nickel and chromium. It was concluded the damage was caused from a stainless-steel orbital debris particle. The aluminum external hard lines are 0.9 mm (0.035 inch) thick in the impacted region. From hypervelocity impact data, the crater depth to wall thickness ratio of 0.52 implied that spall effects were likely on the inside of the line at the point of impact for the deeper crater. A borescope inspection to the line interior was conducted to assess internal damage and a small area of detached spall was found on the inside of the tube under the impact site. This impact nearly put a hole in the external radiator line, which would have caused a leak of Freon coolant, potentially shortening the mission.

Normal and oblique angle tests were conducted with spherical aluminum (Al 2017-T4 alloy) and stainless steel (440C) projectiles. The test data indicates that the ballistic limit particle will increase from 0.6 mm diameter
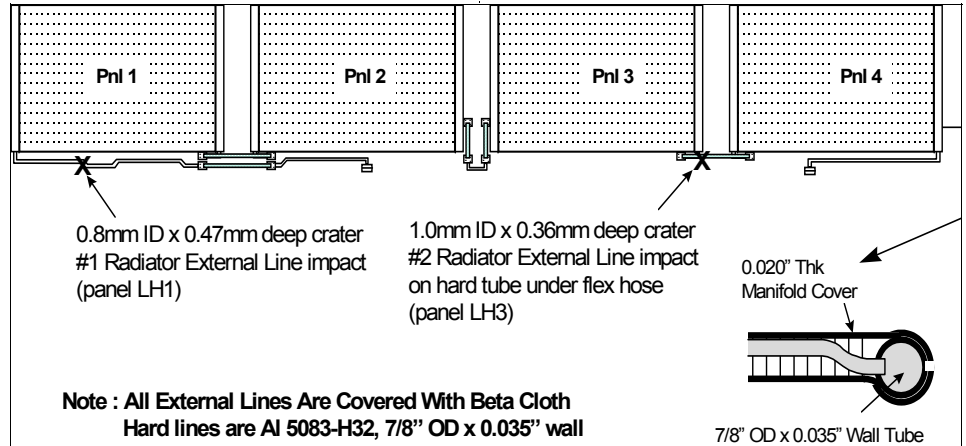

Figure 1. STS-86 location of radiator external line impacts #1 and #2. Detached spall from the inside of the line occurred at impact site #1, and a small bump (attached spall) occurred at site #2. A single-layer beta-cloth sleeve was also penetrated at impact site #1, but no beta-cloth sleeve was present at site #2. Scanning Electron Microscope/X-ray Analysis of impactor residuals indicate that a steel orbital debris impactor was the cause of impact #1, while a meteoroid caused impact #2 [Ref. NASA JSC-28033, "Orbiter Meteoroid/Orbital Debris Impacts: STS-50 through STS-86", August 1998].
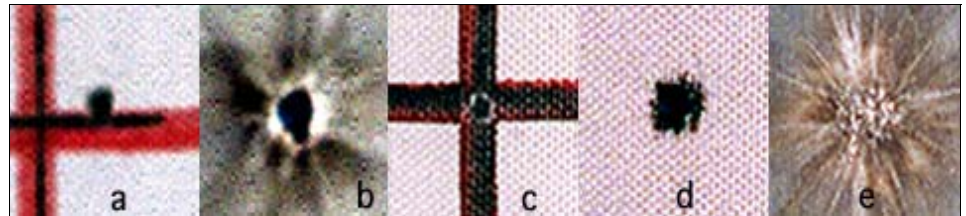

Figure 2. Comparison of results for 1 versus 2 layers Beta-cloth tests.

aluminum particle for a single beta-cloth layer protecting the external line to 0.9 mm diameter aluminum particle for a double beta-cloth protective sleeve at 6.8 km/s and normal angle (0°). Figure 2 illustrates the difference in protection by using one layer of beta-cloth protection (photos a and b) versus two layers of beta-cloth protection (photos c, d and e) when both were tested at 7.0 km/s ±0.2 km/s, 0° using a 1/32-inch Al 2017-T4 spherical projectile. There is a 2.5 mm x 3 mm hole through a 0.032-inch Al 6061-T6 rear wall representing the orbiter radiator external lines located 0.25-inch behind the beta-cloth layer (photo a shows the beta cloth and photo b shows the hole in the line). A similar test with two-beta cloth layers protecting the line resulted in no failure of the line (i.e. no perforation/leak), with damage characterized as multiple craters with maximum size of 0.75 mm diameter in the exterior of the line (photos c and d are of the beta-cloth, photo

e is the rear wall with craters only).

For steel projectiles, the tests indicate the ballistic limit at 6.8 km/s and 45° impact angle is 0.3 mm diameter for a single beta-cloth layer and 0.5 mm diameter for a double beta-cloth layer. For comparison purposes, the ballistic limit (calculated using existing penetration equations) for an external line without beta-cloth is 0.29 mm diameter aluminum (at 6.8 km/s, 0°) and 0.18 mm diameter steel (at 6.8 km/s, 45°).

The Space Shuttle Vehicle Engineering Office, supported by the test data described in this report, determined that a reasonable approach to reduce the penetration risk in subsequent missions would be to add a double-layer beta-cloth sleeve to all external radiator interconnect lines (where the sleeve is sewn with 6.4 mm gap between the beta-cloth layers, and the sleeve is oversized for the line such that

NEWS

Hypervelocity Impact Testing Of Betacloth Covers On Space Shuttle Orbiter Radiator External Lines, Cont'd

(Continued from page 3)
there is on average another 6.4 mm gap between the inner beta-cloth layer and the surface of the external line).

A copy of the full report of the study, *Hypervelocity Impact Testing Of Beta-cloth Covers On Orbiter Radiator External Lines* (JSC 28524), can be obtained from the HITF document archive at http://hitf-archive.jsc.nasa.gov/ or from the HITF on-line library at http://hitf/hitfpub/main/index.html.

References
1. Crews, J.L. and E.L. Christiansen, *The NASA JSC Hypervelocity Impact Test Facility (HITF)*, AIAA 92-1640, 1992.
2. Christiansen, E.L., *Orbiter Meteoroid/Orbital Debris Impacts: STS-50 (6/92) through STS-86 (10/97)*, NASA JSC-28033, August 1998.
3. Nguyen, S. and A. Richards, *External Radiator Line Protection from Micrometeoroid Orbital Debris (MMOD) Impacts*, ORB MCR 19257, March 24, 1998. ❖

New Report on Hubble Space Telescope Impact Damage

The Image Science and Analysis Group at the NASA Johnson Space Center has just released its latest assessment of small particle damage to the HST in *Survey of the Hubble Space Telescope Micrometeoroid and Orbital Debris Impacts From Space Shuttle Service Mission 3A Imagery* (JSC-29539). Prepared primarily by David Bretz and the late Leif Anenson, the report characterizes the results of a special investigation of HST photographs from the December 1999 mission of STS-103 to identify high velocity impact features. A similar analysis was performed following the second HST servicing mission by STS-82 (see *Survey of the Hubble Space Telescope Micrometeoroid and Orbital Debris Impacts from Service Mission 2 Imagery*, JSC-28472, 1998).

During the STS-103 mission the Electronic Still Camera (ESC) was used from inside the Space Shuttle crew cabin to map all visible areas of the body of HST using a 80-200 mm lens at full zoom (200 mm) and to image selected areas with the 400 mm telephoto lens. Astronaut Scott Kelly was the primary survey photographer, who underwent preflight training for this mission task. A total of 99 images (50 with the 200 mm lens and 49 with the 400 mm lens) were taken from the aft flight deck. Many of these images were selected for special particle impact analysis.

In all, 571 impact features (strikes) were selected for characterization and measurement: 398 in the 200 mm lens images and 173 in the 400 mm lens images. Where possible, the dimensions of both the central hole and the outer delamination ring were measured. The most prevalent hole size seen in the 200 mm lens images was 2-3 mm, but the higher resolution 400 mm lens images yielded a majority of hole diameters in the 1-2 mm range. The delamination ring diameters typically are twice the size of the associated hole.

One of the most important metrics for determining the flux of the particle environment is the density (number per square meter) of impacts. Average impact densities of about $45/m^2$ were found on the −V3 quadrant of HST. This is a cumulative effect over almost 10 years in Earth orbit. Unfortunately, micrometeoroid and orbital debris impacts cannot be differentiated in the images. Therefore, statistical techniques, taking into account the mean densities of micrometeoroids and orbital debris and their effects on hypervelocity impact morphology, will need to be applied to distinguish the probable populations. ❖
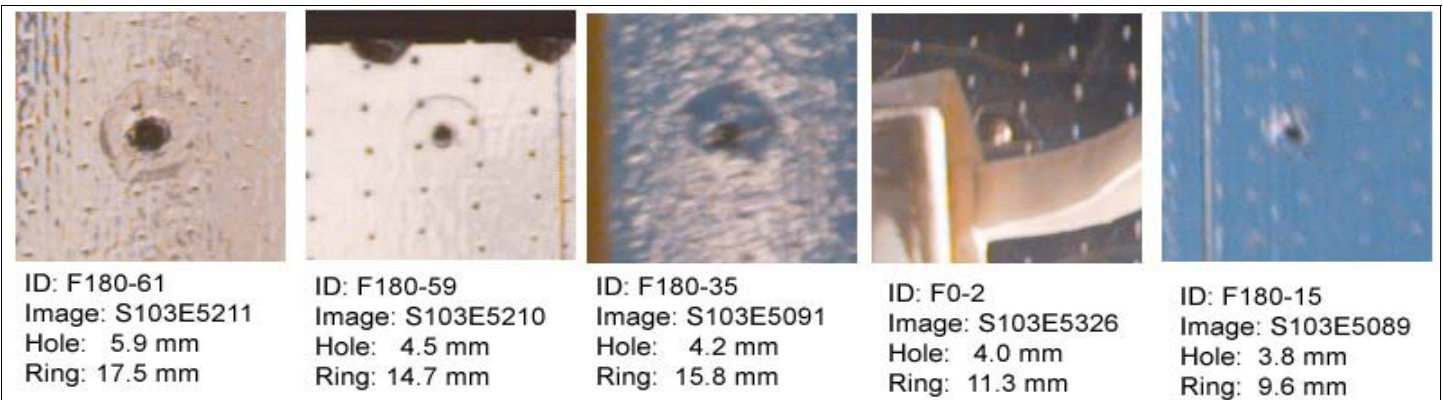
ID: F180-61 Image: S103E5211 Hole: 5.9 mm Ring: 17.5 mm
ID: F180-59 Image: S103E5210 Hole: 4.5 mm Ring: 14.7 mm
ID: F180-35 Image: S103E5091 Hole: 4.2 mm Ring: 15.8 mm
ID: F0-2 Image: S103E5326 Hole: 4.0 mm Ring: 11.3 mm
ID: F180-15 Image: S103E5089 Hole: 3.8 mm Ring: 9.6 mm

Figure 1. Five HST impact sites photographed with 400 mm lens.

Visit the NASA Johnson Space Center Orbital Debris Website

http://www.orbitaldebris.jsc.nasa.gov

Project Reviews

LEGEND – The Next Generation NASA Orbital Debris Evolution Model

J.-C. Liou, P. Anz-Meador, D. Hall, P. Krisko, and J. Opiela

To continue to improve our understanding of the orbital debris environment, the NASA Orbital Debris Program Office has initiated an effort to develop a new debris evolution model to replace EVOLVE. The first generation of the EVOLVE model was written in 1986 (Reynolds 2001). Over the years, several major upgrades have been completed and implemented into the main model and supporting models (*e.g.*, Reynolds and Eichler 1995, Reynolds *et al*. 1998, Krisko *et al*. 2000). Basically EVOLVE is a one-dimensional orbital debris model describing the Low Earth Orbit (LEO) environment between 200 and 2,000 km altitude. For more than a decade it has been a leading model providing critical insights into the orbital debris environment. It was also the tool supporting the development and publication of NASA Safety Standard 1740.14 in 1995.

The motivations to build a new model to replace EVOLVE are twofold. First, a one-dimensional description/treatment in altitude of the debris environment is not adequate. The spatial density of debris at the same altitude can vary significantly as a function of latitude. In addition, populations such as Sun-synchronous, Molniya, and objects in Geosynchronous Earth Orbit (GEO) all have strong longitudinal dependence. To describe the orbital debris environment correctly and to analyze its future behavior (such as collisions) properly, a multi-dimensional model is needed. Second, as the debris populations continue to grow, there is a need to build a full-scale debris model describing the near-Earth environment from LEO to GEO and above.

LEGEND, a LEo-to-Geo ENvironment Debris model, is a full-scale three-dimensional debris evolution model. It covers the near-Earth space between 200 and 50,000 km altitude, including LEO (200 to 2,000 km altitude), Medium Earth Orbit (MEO, 2,000 to 34,000 km altitude), GEO (34,000 to 38,000 km altitude), and super-GEO (38,000 km and above) regions. The model is capable of providing debris characteristics (size distribution, spatial density distribution, velocity distribution, flux, *etc*.) at a given time or as functions of time, altitude, longitude, and latitude. LEGEND includes a historical simulation component (1957 to 2000) and a future projection component. The historical part of the model has been completed while the future projection module is being developed currently.

The main function of the LEGEND historical component is to reproduce the debris environment between 1957 and 2000. The model utilizes a recently updated historical satellite launch database, two efficient state-of-the-art propagators (PROP3D, GEOPROP), and a new NASA satellite breakup model. The overall program structure and the input and output options are optimized to allow reasonable execution time and manageable file storage space. Additional analysis modules are also developed to visualize the outputs and to enable easy comparisons with existing ground-based debris observations. The main program is written in FORTRAN 90 with additional analysis tools written in IDL and SuperMongo.

The top-level program logic of LEGEND is very similar to other debris evolution models, such as EVOLVE and IDES (Walker *et al*. 1996). Source mechanisms, including satellite launches and breakup events, add objects to the environment while sink mechanisms, including decay and deorbit, remove objects from the environment. Major perturbations that affect the orbital evolution of objects are included in the program. For GEO objects, solar and lunar gravity, solar radiation pressure, the Earth's
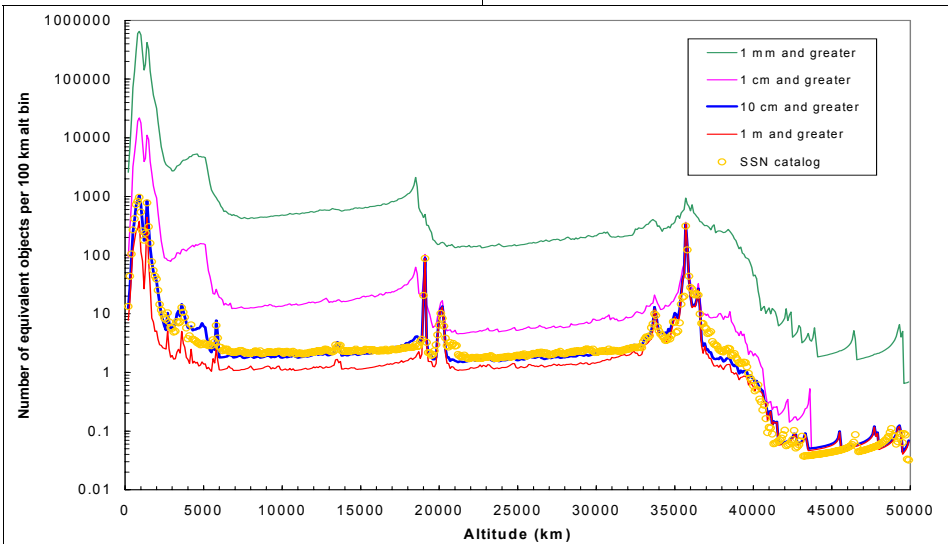

Figure 1. One-dimensional distributions, of objects of 4 different size thresholds, between 200 and 50,000 km altitudes.
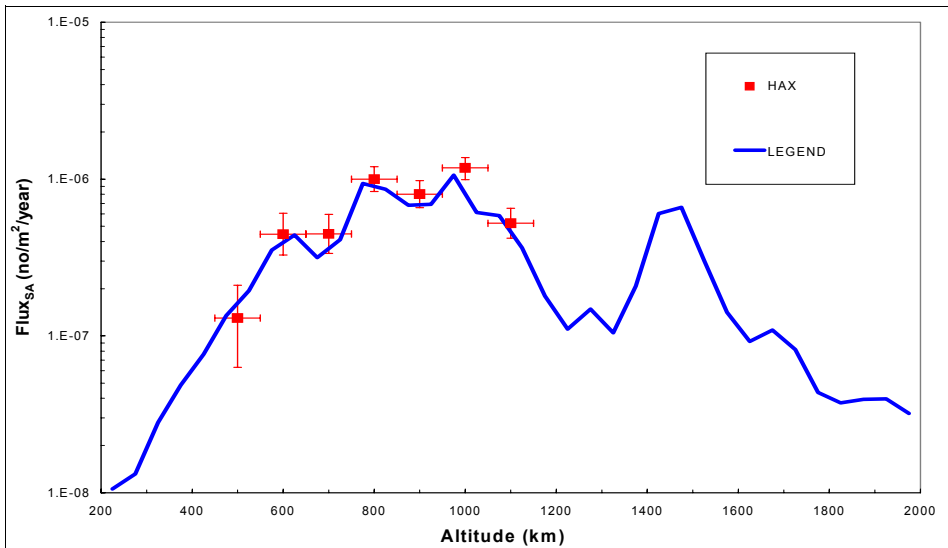

Figure 2. LEGEND prediction versus HAX radar observations for objects 10 cm and greater (in 1999).

Project Reviews

LEGEND – The Next Generation NASA Orbital Debris Evolution Model, Cont'd

zonal harmonics (J_2, J_3, J_4), and the Earth's sectorial harmonics ($J_{2,2}$, $J_{3,1}$, $J_{3,3}$, $J_{4,2}$, $J_{4,4}$) are included. For LEO and MEO objects, atmospheric drag, solar and lunar gravity, solar radiation pressure, Earth's shadow effect, and Earth's zonal harmonics (J_2, J_3, J_4, J_2^2) are included.

LEGEND outputs debris distributions in 1-D (altitude), 2-D (altitude, latitude), and 3-D (altitude, latitude, longitude) formats at a given time or as functions of time. The orbital element arrays maintained by the program are processed in several modules analyzing debris characteristics in multi-dimensions. In general, the altitude-latitude 2-D distributions are sufficient for debris environment definition and characterization. The exceptions are GEO objects or objects with special types of orbits (*e.g.,* Sun-synchronous or Molniya) where the dependence in longitude may be needed to better describe their distributions in space. Figure 1 shows the number of objects per 100 km altitude bin from the end of LEGEND historical simulation (the end of 2000). The four curves, from top to bottom, correspond to objects 1 mm and greater, 1 cm and greater, 10 cm and greater, and 1 m and greater, respectively. The same distribution derived from the Space Surveillance Network (SSN) catalog is represented by open circles in the figure. Note that the Sodium-Potassium (NaK) droplets and Solid Rocket Motor (SRM) ejecta modules have not been implemented into LEGEND. Also, the NASA breakup model is being reviewed currently for breakup fragments smaller than 10 cm. The 1 mm and 1 cm curves will be updated in late 2002 when all modules are in place. Figure 2 shows the LEGEND-predicted surface area flux of objects 10 cm and greater as would be observed by the HAX radar in 1999. In both cases the model predictions compare well with the actual data for objects 10 cm and greater.

LEGEND is a three-year project (FY01-03) supported by the NASA Orbital Debris Program Office. The historical part of the model has been completed. The future projection module, including a three-dimensional collision model, NaK and SRM ejecta modules will be developed in FY02. Validation and verification of LEGEND will take place in early 2003 before the completion of the model in September 2003.

References
1. Krisko, P.H. *et al.,* 2000. Lockheed Martin Space Operations Report LMSMSS-33020.
2. Reynolds, R.C., 2001. In "Space Debris 2000", IAA 00-6.6.08, 315-322.
3. Reynolds, R.C. and P. Eichler, 1995. Adv. Space Res. 16, 127-135.
4. Reynolds, R.C. *et al.*, 1998. Lockheed Martin Space Operations Report LMSMSS-32532.
5. Walker, R. *et al.*, 1996. Space Flight Mechanics, Vol. 93, 201-220. ❖

Orbital Evolution of Cloud Particles from An Explosion in Near-GEO

T. Hanada and M. Matney

Current search strategies for telescopes observing the Geosynchronous Earth Orbit (GEO) environment are designed around the known orbital distribution of catalogued objects. However, the majority of catalogued objects are believed to be intact spacecraft and rocket bodies. These strategies may neglect small debris populations from energetic explosions that have occurred in or near GEO. If there have been breakups in GEO, the explosions may have put the debris into orbits that are significantly different from those in the catalogue. Consequently, observation plans optimized for the catalogued population may not be optimized for any unseen debris populations.

We will present the actual near-synchronous US Titan IIIC Transtage explosion of 21st February 1992 to demonstrate the above-mentioned effect and make some observations on how to implement future search strategies. We simulate this transtage explosion using the latest NASA breakup model to create five hundred breakup fragments greater than about 2 cm in size, and then propagate the fragment cloud.

In addition to the spherically symmetric gravitational force of the Earth, a number of perturbing accelerations affect the orbit of a GEO or near-GEO object. The forces that need to be considered for evolution of cloud particles from explosion are: 1) the non-spherical part of the Earth's gravitational potential, 2) gravitational attractions due to the Sun and Moon (approximated as point masses), and 3) solar radiation pressure. For this study, we omitted solar radiation pressure: not because it is unimportant for this type of analysis, but because we wanted to concentrate only on the primary orbit perturbations.

The lunar and solar gravitational attractions combined with the Earth's zonal harmonics of the Earth's gravitational potential drive a precession of a geosynchronous satellite's orbit plane. This precession generates a 54-year cycle of orbital inclination with respect to the equator, yielding a maximum inclination of 14 to 15 degrees (the precise value varies from cycle to cycle). What is happening is that the orbital angular momentum vector for the satellite's orbit is precessing about an axis displaced approximately 7.4 degrees from the Earth's rotation axis towards the ecliptic pole. The cycles of orbital inclination and right ascension of the ascending node caused by this precession can be found in Friesen et al. (1993). A plot in the coordinate system given by $x = i \times \cos\Omega$ and $y = i \times \sin\Omega$ (where i represents orbital inclination and Ω represents right ascension of the ascending node) represents the orbital angular momentum direction, or orbit pole, as seen from celestial north. We are focusing on the precession of the orbit planes of the particles relative to that of parent object.

Figure 1 demonstrates orbital evolution of the debris cloud from the near-synchronous US Titan IIIC Transtage explosion. In the figure, filled circles represent 1-year interval projection of the parent object's "unexploded" orbit. The cloud particles begin in a straight line on the x-y graph, then the pattern is deformed with the cloud's evolution maintaining distinctive patterns centering around the parent object long after the explosion has occurred. Note that the particles in the cloud have different cycling periods, not just the 54-year period of a typical GEO object.

The tangential components of the perturbing accelerations due to the Earth's tesseral harmonics, involved in the non-spherical part of the Earth's gravitational potential distributed in terrestrial longitude, are smaller than other perturbations by a factor of one thousand. However, the resonance effect on 24-hour geosynchronous orbits induces a very slow motion, librating around the stable longitudes with a period of about 800 days and amplitude of nearly 90 degrees. The primary tesseral harmonic is designated by J_{22}. The longitude of symmetry of the J_{22} harmonics denoted by λ_{22} is determined from observations and has a typical

Project Reviews

Orbital Evolution of Cloud Particles from An Explosion in Near-GEO, Cont'd

(Continued from page 6)

February 21, 1992

January 1, 2000

January 1, 2010

January 1, 2020

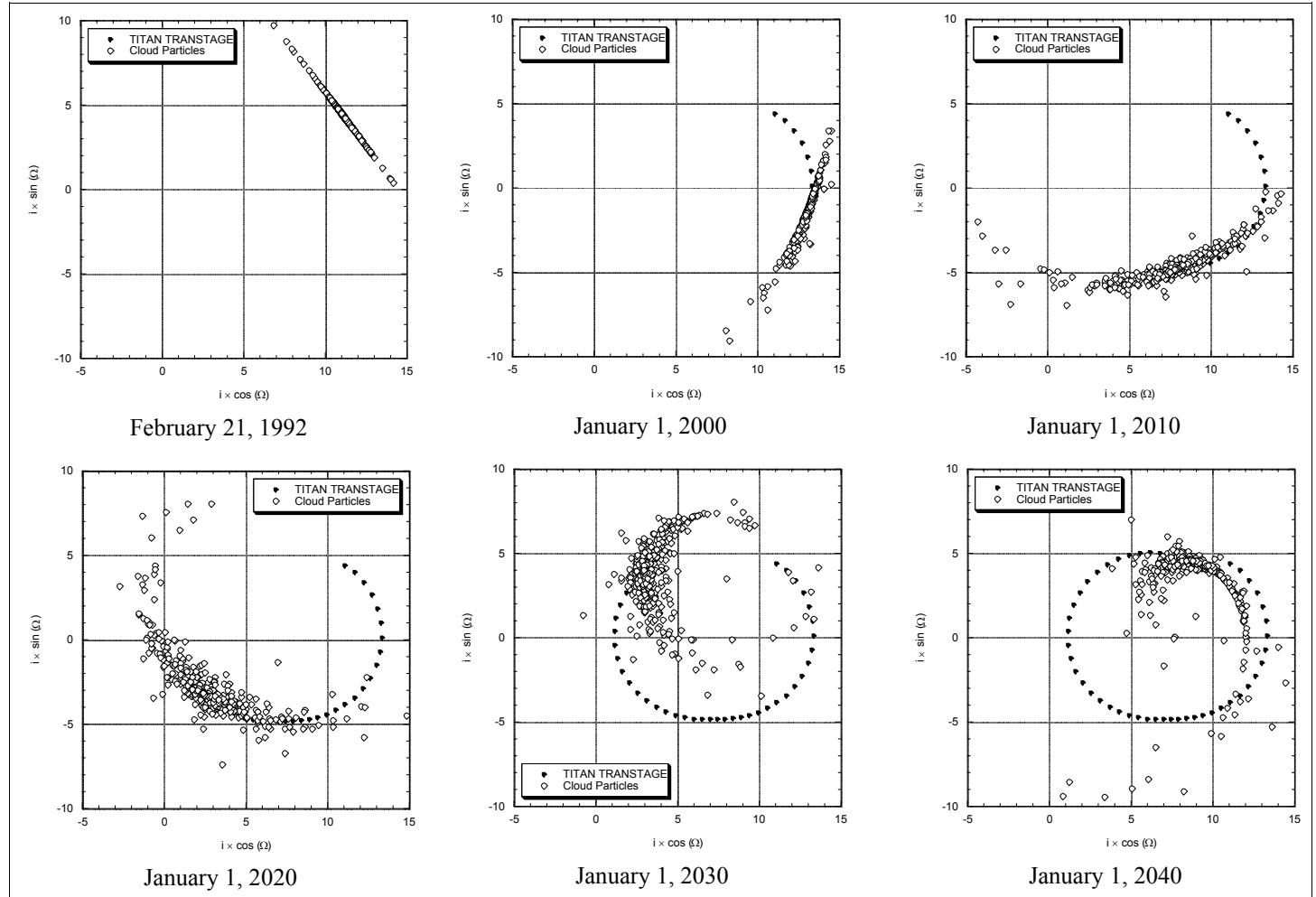January 1, 2030

January 1, 2040

Figure 1. Simulated Evolution of Debris Cloud from Near-Synchronous US Titan IIIC Transtage Explosion.
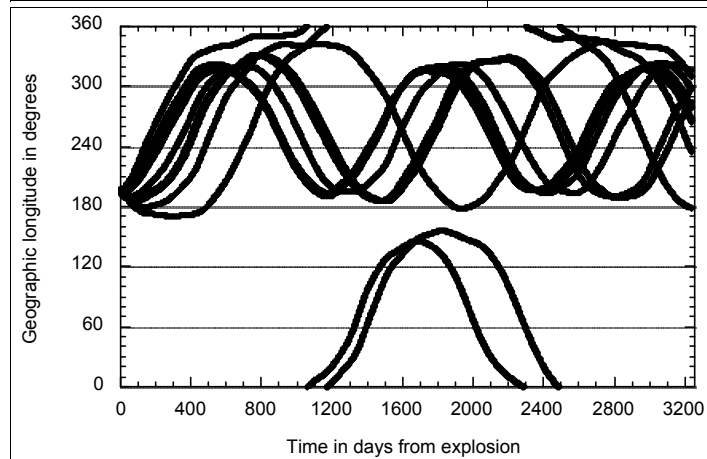

Figure 2. Simulated Longitude Evolutions of Librating Cloud Particles from Near-Synchronous US Titan IIIC Transtage Explosion.

value of −14.7 deg. The equilibrium points are divided into stable (75.1° East and 105.3° West) and unstable (11.5° West and 161.9° East) longitudes. We are also interested in how cloud particles get trapped in this longitude drift evolution.

Figure 2 demonstrates the longitude drift evolution of librating cloud particles. Only ten cloud particles out of five hundred are affected by the resonance effect of the 24-hour geosynchronous orbit. Eight cloud particles librate centered around the Western stable point, while two particles librate around both stable points. Note that the particles spend much of their time "paused" near the unstable libration points.

We simulated the near-synchronous US Titan IIIC Transtage explosion of 21 February 1992 using the latest EVOLVE 4.0 breakup model. Then we propagated the evolution of cloud particles from this transtage explosion for long periods (about 50 years). In the coordinate system we adopted here, breakup clouds in near-GEO maintain distinctive patterns long after the explosion has occurred. "Normal" GEO objects – intact objects that are left in or near GEO with minimal delta-velocity – follow distinctive patterns in their evolution, but these

Project Reviews

Orbital Evolution of Cloud Particles from An Explosion in Near-GEO, Cont'd

(Continued from page 7)
breakup cloud particle orbits can evolve in quite different ways. GEO search strategies should consider the possibility of debris clouds with orbital elements different from the intact population distribution, especially at inclinations that exceed the typical 15° inclination limit of "normal" GEO objects. Only a fraction of breakup debris particles appear to become trapped in librating orbits. Nevertheless, searches concentrating near the unstable libration points might reveal concentrations of debris particles.

References

1. L. J. Friesen, D. J. Kessler, and H. A. Zook, "Reduced Debris Hazard Resulting From Stable Inclined Geosynchronous Orbit," *Avs. Space Res.*, Vol.13, No.8, 1993, pp.231-241. ❖

Preliminary Results from the NASA AMOS Spectral Study (NASS)

K. Jorgensen

The physical characteristics of debris are taken into consideration in the space environment models, the building of shields, and provide base work for future studies. Some of these characteristics are assumed currently, including material type. Using low-resolution spectroscopy, researchers have determined the material type of man-made orbiting objects in both low Earth orbits (LEO) and geosynchronous Earth orbits (GEO). By comparing absorption features of spectra collected on the 1.6-meter telescope at AFRL Maui Optical Site (AMOS) with a laboratory database of spacecraft material spectra, the material type of known objects was determined. Using the spectral range of 3500 – 9000 angstroms, researchers can separate materials into classification ranges.

NASS (NASA AMOS Spectral Study) began observations in May 2001, with eight nights of data collection. The objects were observed a minimum of three times constrained by the orbit and inclination of the object. Twenty-two rocket bodies (R/Bs) were observed with both a blue and red filter during the May observing run. AMOS supplied spectral data of the objects corrected for background and the atmosphere through IRAF routines. Reduction of the data was completed at NASA JSC using Specpr, an in-house program supplied by the United States Geological Survey (USGS), and MATLAB scripts. Both the laboratory and remote sample have been scaled to approximately 6000 angstroms so that the samples can be compared more easily as well as allowing the blue and red spectra to be on a continuous line.

Each material type will show a different spectrum based on its composition. Figure 1 shows a LEO R/B overlaid (line with more noise) with laboratory samples (smoother line) in an attempt to characterize the material type of the R/B. The feature seen near 4000 angstroms is due to white paint and is labeled on the figure as "white paint". Labeled as "aluminum" near 8400 angstroms is a strong
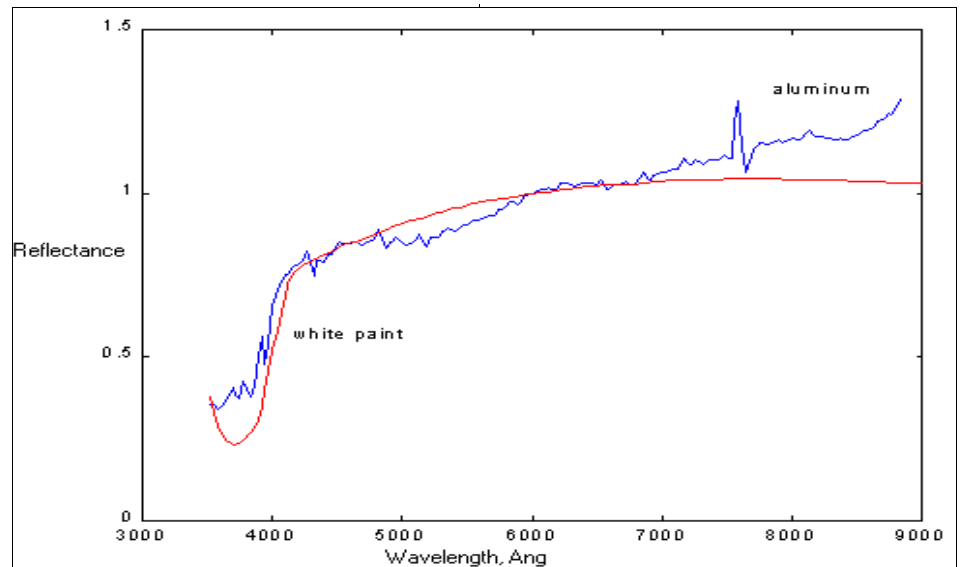

Figure 1. LEO R/B spectra compared to a Laboratory Sample of Flown White Paint from LDEF
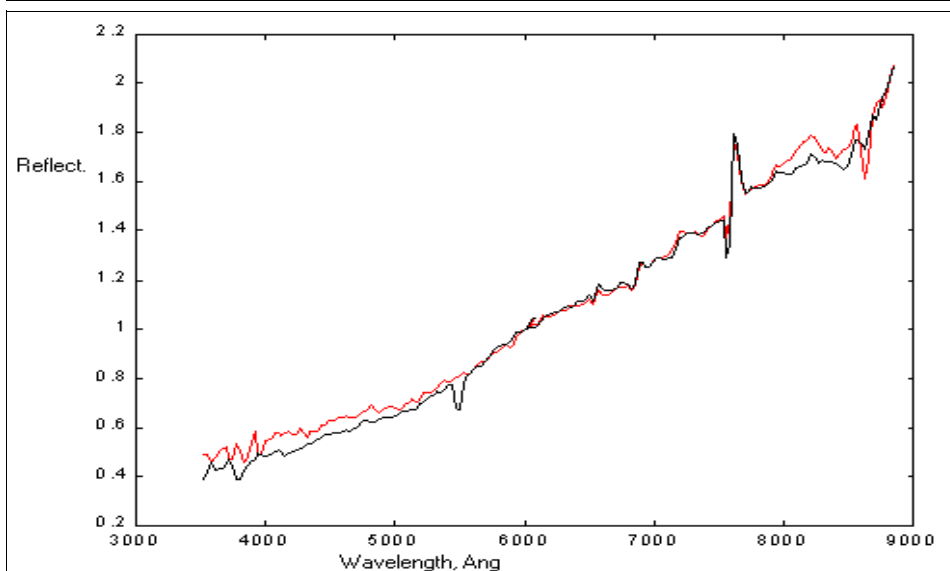

Figure 2. Similar R/Bs Observed on the Same Evening

Project Reviews

Preliminary Results from the NASA AMOS Spectral Study (NASS), Cont'd

(Continued from page 8)

aluminum feature. The laboratory sample is white paint flown on the Long Duration Exposure Facility (LDEF). The sample was in the ram direction and was exposed to 5.7 years of direct sun [1].

One area that the samples do not match is the rise in reflectance in the remote sample from approximately 7000 - 9000 angstroms. Currently, the best theory for the increase is tiny granulations are increasing the specular reflectance of the object in that region. This increase is seen in some asteroid samples, due mostly to small pieces of iron, as well as the returned lunar samples. Future studies will be conducted to try and simulate this phenomenon in the lab. One solution to deal with the increase, which was used with the lunar samples, is to divide out the continuum (slope) to better observe the features in this region. By dividing out the continuum, researchers can tell the difference between small features currently being overshadowed by the large increase due to the iron. Once the continuum has been divided from the R/B, the authors believe the lines will match the sample with greater accuracy. Figure 1 shows that material identification is possible with this technique.

In addition to determine the material type of orbiting objects, NASS can be used for determining degradation of satellites as well as determining mistaged objects. R/Bs with similar paint schemes will depict similar features in the spectra and currently, the author has not found a correlation between phase angle and shape of the spectrum. Therefore, R/Bs made by similar countries will look similar. Whether or not there is a dependence on the launch date is still unknown at this time. Further studies will explain this possibility. Shown in Figure 2 is a comparison between two similar R/Bs launched five years apart and it has not been determined
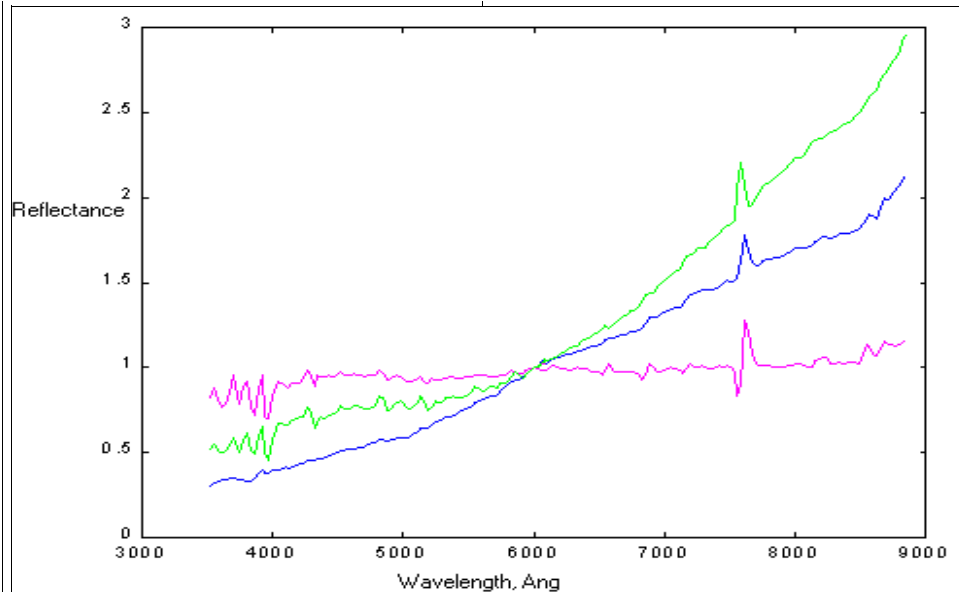

Figure 3. Three different R/Bs Observed on the Same Evening

whether or not this is enough of a difference in time to show variations in the spectra. Notice that the absorption features are located in similar positions and the shape of the spectra are very similar. Figure 3 shows three different R/B's observed on the same evening. This picture shows that R/B's composed of differing materials can be separated from one another.

More observations are on the schedule using the 1.3-meter telescope at AMOS as well as beginning observations using the 3.67-meter telescope at the same site. Observations will continue with the R/Bs and in the future will include intact satellites, large debris fragments, and eventually, smaller debris. Finding an explanation for the increase in the reflectance in the red is of high priority. Material identification of the current observations will continue as

well as determining whether the effects of space weathering and other age dependent factors can be seen as well with this technique.

References

1. Jorgensen, K., *Determining the Material Type of Orbital Debris Using Reflectance Spectroscopy*, Ph.D. Thesis, University of Colorado, Boulder, May 2000.   ❖

Doppler Inclination Estimates from Haystack Measurements of the Debris Environment

E. Stansbery and M. Matney

The Orbital Debris Program Office at Johnson Space Center has been statistically sampling the low earth orbit debris environment using the Haystack Long Range Imaging Radar since late 1990. During these measurements, the radar is pointed in a specified direction and debris objects pass through the radar's field-of-view (FOV) without the radar trying to track the object. The radar is operated in a pulsed mode

and the returns from each individual pulse are recorded for later analysis. These returns include the azimuth and elevation difference channels which can be used to locate where the object is in the radar beam. Orbital elements can be estimated by using the path through the beam, the range to the target, and the range rate which is derived from the Doppler shift between the transmitted frequency and the received frequency reflected by the target

debris. Unfortunately, there are challenges to implementing this technique in the real world.

One of these challenges is contamination of the signals by noise. The returns from twelve pulses are non-coherently integrated to produce a signal-to-noise ratio (SNR) to determine valid detections with an acceptable false alarm rate. No integration is possible for the azimuth and elevation difference channels

Project Reviews

Doppler Inclination Estimates from Haystack Measurements of the Debris Environment, Cont'd

(Continued from page 9)

since the individual returns are used for locating the object in the beam. Therefore, for low SNR detections which require integration to bring them out of the noise, the difference channels will often still be dominated by noise.

A second challenge is contamination of the signals by crosstalk. Haystack transmits right hand circular polarization and receives left hand circular polarization (called principal polarization, or PP) in the sum and difference channels along with a right hand sum channel (called orthogonal polarization, or OP). The OP difference channels are also received but are terminated in the feed horn. There is typically 26-30 dB or more isolation between the OP and PP channels. However, for large objects which have a high OP return signal, contamination, or crosstalk, into the PP difference channels can and does occur producing errors in determination of the location of the object in the radar beam.

In order to determine the path through the antenna beam, the individual estimates of location are fit to a straight line using a weighted (by SNR) least squares fit. Inclination is determined by the direction of the straight line. Eccentricity is determined by a combination of the range and range rate of the target and of the angular velocity of the object through the beam. Unfortunately, eccentricity is very sensitive to angular velocity. For our data, we have found that the estimates of eccentricity are not acceptable for use. We have also found that large errors in the inclination determination can also exist for SNRs below about 15 dB. We have called this traditional method for estimating inclination – Monopulse Inclination.

Inclination can also be estimated by combining the range rate with the slant range to the target for a non-vertical staring radar and assuming a circular orbit. Approximately 75% of cataloged objects have eccentricities below 0.1, so the circular orbit assumption should work well for a large majority of detected objects. To understand how Doppler can estimate inclination, consider the case with Haystack pointing due south (azimuth 180°) at an elevation angle 10° above the horizon. The radar is located at about 42.6° N. Latitude. At a slant range of 1160 km, the antenna beam is centered at 300 km altitude at a N. Latitude of 32.7°. As the slant range increases, the radar beam crosses higher altitudes at latitudes further south. At 1695 km slant range the beam is at
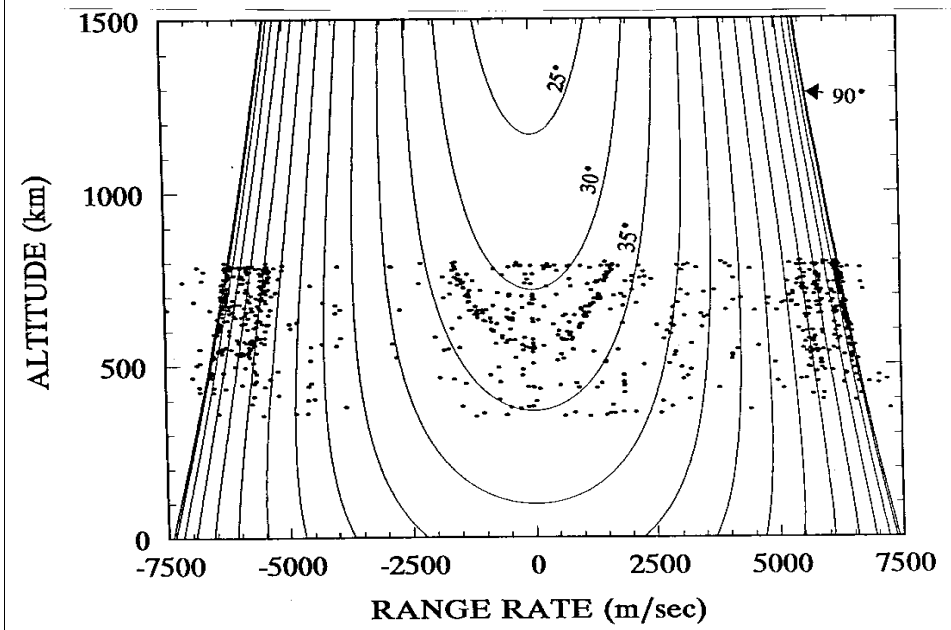

Figure 1. Altitude – Range Rate plot for data collected at Haystack using pointing angles of 20° EL and 180° AZ (South) with overlays of inclination calculated from the Doppler assuming circular orbits.
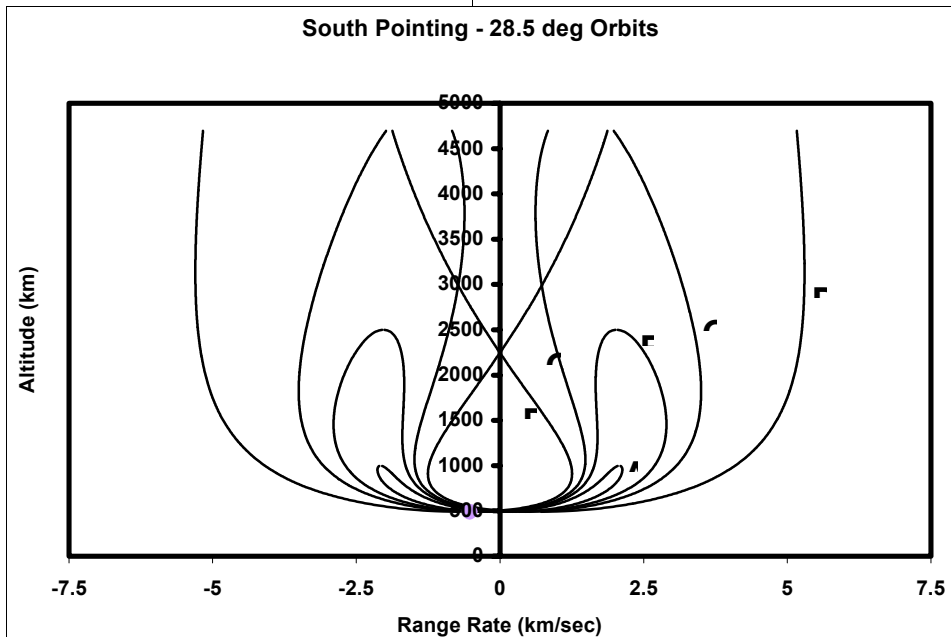

Figure 2. Altitude – Range Rate plot of 28.5° elliptical orbits as seen from Haystack using pointing angles of 10° EL and 180° AZ (South).

500 km altitude and 28.5°. At 2155 km slant range, the beam is at 700 km altitude and 25.1°.

Now consider the near sinusoidal ground track of a low earth satellite in a circular orbit on a Mercator projection of the Earth. At the

Project Reviews

Doppler Inclination Estimates from Haystack Measurements of the Debris Environment, Cont'd

(Continued from page 10)
northernmost point of the orbit, the ground track runs east-west and has no north-south component (Also, the geocentric latitude at this northernmost point is equal to the inclination of the orbit). If the altitude of the satellite is such that it crosses through the beam of the radar at this northernmost point in its orbit, it will have no north-south motion and there will be no Doppler shift in the received signal at the radar. If the satellite is at a higher altitude (but same inclination) it can only pass through the radar beam at a latitude farther south. At this location, the satellite will have some north-south motion and will, therefore, produce a radar return with some Doppler shift. For orbits of the same inclination, the radar will see an increasing Doppler shift as the altitude of the orbit increases corresponding to a radar beam intersection point moving further south.

Figure 1 shows slant range and range rate for detections from Haystack pointing south at an elevation of 20° above the horizon. Also shown are the theoretical slant range-range rate curves for different orbit inclinations assuming circular orbits. The concentrations of detections seen in this plot can be explained as families of near-circular orbits with similar inclinations spread over some altitude range.

What about non-circular orbits? Certainly Haystack is detecting non-circular orbits. It is just that Haystack is not detecting enough objects from any one highly-elliptical orbit to create any easily-discernable patterns. Part of this is due to the fact that typical GEO-transfer orbits (GTOs) spend only a tiny fraction of their time in altitudes that Haystack can easily see. Therefore, even if there is a significant population of centimeter-size debris in elliptical orbits, the number of detections will probably be too low to make clear patterns. In addition, breakups of objects in high-eccentricity orbits tend to scatter the debris into orbits with a variety of perigee altitudes. This effect is further enhanced by perturbations from the Sun and Moon that cause the perigees of the different debris orbits to oscillate. These effects spread out the "patterns" in a range/range-rate plot making it difficult to see clear families. Some orbits, such as 7 degree GTOs simply cannot be seen easily by Haystack. Others, such as Molniya orbits, have their perigees in the southern hemisphere, and are simply not at low altitudes over the northern hemisphere. All these effects tend to make elliptical orbits particularly elusive to Haystack detection.

For those highly-elliptical orbits that Haystack can sample, it has been speculated that much of the centimeter sized debris comes from aluminum oxide solid rocket motor (SRM) slag. This slag would be ejected both during
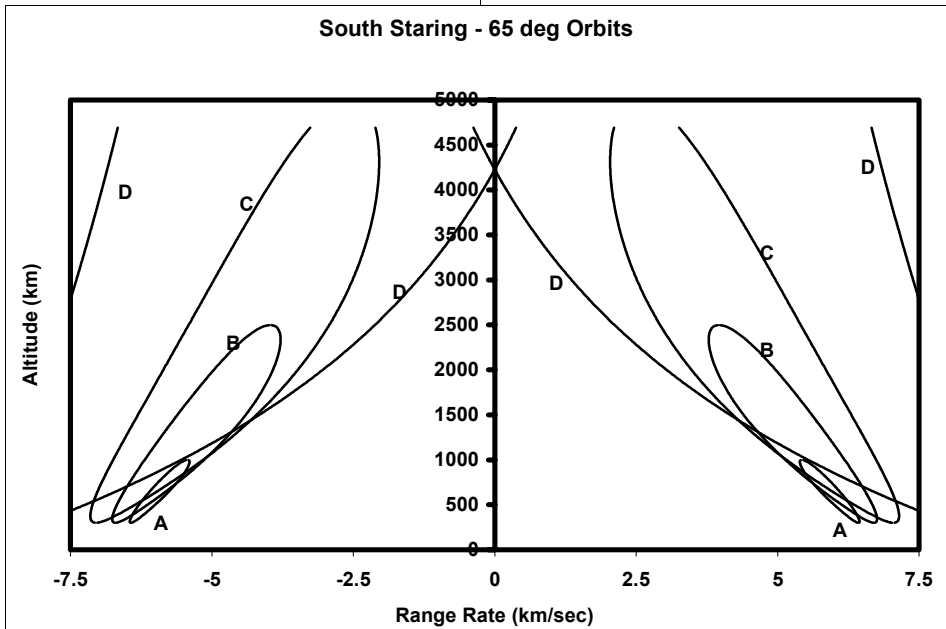

Figure 3. Altitude – Range Rate plot of 65° elliptical orbits as seen from Haystack using pointing angles of 10° EL and 180° AZ (South).
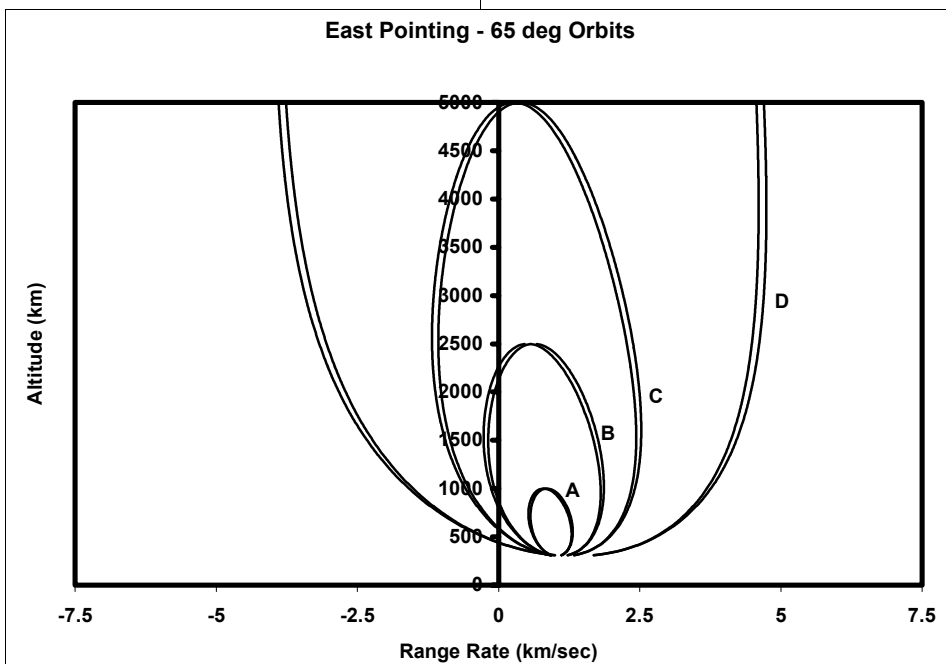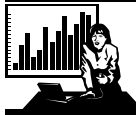

Figure 4. Altitude – Range Rate plot of 65° elliptical orbits as seen from Haystack using pointing angles of 75° EL and 90° AZ (East).

Project Reviews

Doppler Inclination Estimates from Haystack Measurements of the Debris Environment, Cont'd

and after a solid rocket motor firing for injection of a payload into a geo-transfer orbit. During the firing, slag would be ejected at high

	Perigee	Apogee
A	300	1000
B	300	2500
C	300	5000
D	300	36000

Table 1. Apogee and perigee for orbits plotted in Figure 2-4.

velocity from a parent body with a continuously changing eccentricity. Only large amounts of slag released at low velocities after SRM burnout would have any possibility of forming a detectable stream at Haystack.

In order to determine what such a stream might look like, Mark Matney has written a program which calculates the slant range (or in this case altitude) – range rate plots for elliptical orbits. Figure 2 shows 28.5° orbits of varying eccentricities as seen from Haystack at a staring angle of 10° EL and 180° AZ (south). Figure 3 shows a 65° orbit for the same staring angle. NASA also uses a staring angle of 75° EL and 90° AZ (east). At this angle, 28.5° orbits are never visible. Figure 4 shows a 65° orbit for

the 75°/90° pointing angle. Table 1 gives the apogee and perigee for the orbits plotted in Figures 2-4.

In summary, although Haystack is probably detecting a wide distribution of objects in eccentric orbits, no concentration of detections exist which would identify a single highly populated, highly eccentric orbit. ❖

Reentry Survivability Analysis of the Earth Observing System (EOS)-Aura Spacecraft

W. Rochelle and R. O'Hara

The National Aeronautics and Space Administration (NASA) Goddard Space Flight Center (GSFC) Earth Observing System (EOS)-Aura spacecraft is currently scheduled for launch in July 2003. In accordance with NASA Policy Directive 8710.3, GSFC performed a reentry analysis of the Aura spacecraft using the NASA Lyndon B. Johnson Space Center (JSC) Debris Assessment Software (DAS). The GSFC DAS results showed the Aura spacecraft to be non-compliant with NASA Safety Standard 1740.14 Guideline 7-1, which requires the surviving debris of an uncontrolled spacecraft reentry to produce a risk to ground population no greater than 1:10,000. In response to the results, GSFC requested an analysis be performed using the higher fidelity Object Reentry Survival Analysis Tool (ORSAT), developed by JSC and Lockheed Martin Space Operations.

The approximately 2400 kg Aura satellite will be used to analyze Earth's lower and upper atmospheres, tracking changes in the ozone as well as providing valuable information on the dynamics of the various atmospheric layers and how they affect us here on Earth. Four major instruments on Aura will be used to perform the research: the High-Resolution Dynamics Limb Sounder (HIRDLS), Tropospheric Emission Spectrometer (TES), Microwave Limb Sounder (MLS) and Ozone Monitoring Instrument (OMI). Figure 1 shows a pictorial representation of the Aura spacecraft and the location of the main instruments.

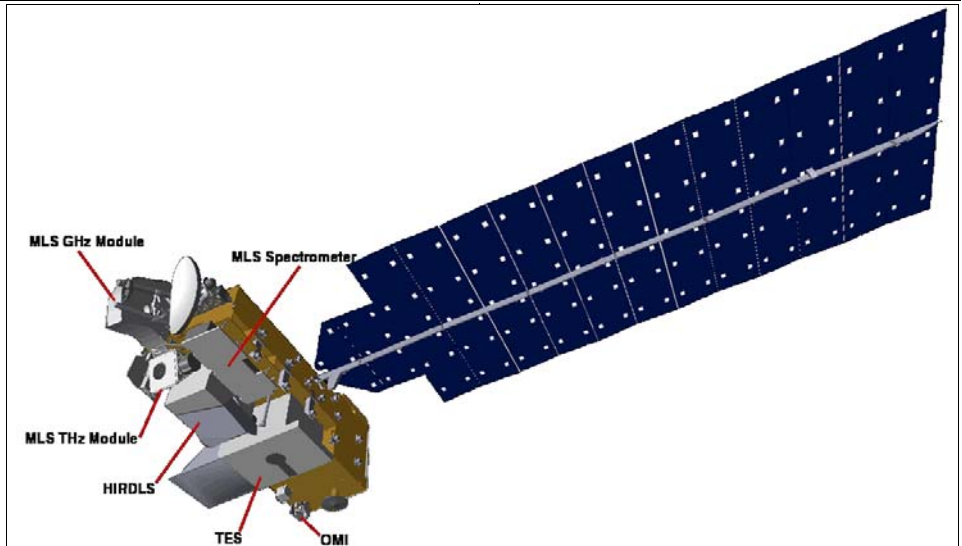Eventually the orbital decay of the Aura

Figure 1. EOS-Aura satellite showing instrument locations (courtesy of the GSFC EOS-Aura website: http://eos-chem.gsfc.nasa.gov/index.html)

spacecraft will cause it to reenter the Earth's atmosphere, resulting in break-up and demise of most of the spacecraft components. However, due to the mass, size, and material properties of some of the components, there is an increased possibility of those components surviving the atmospheric reentry and posing a safety risk to the ground population. In the reentry analysis performed using ORSAT, entry interface for the Aura spacecraft was assumed to be 122 kilometers, with initial breakup occurring at 78 kilometers. A total of 132 components were analyzed with ORSAT,

including those making up the four major Aura instruments for mapping data on the Earth's atmosphere. Detailed component properties were obtained and used to model each individual component in ORSAT. All of the aerodynamic mass was modeled or accounted for in the analysis. Of the 132 components, only 6 survived (9 total when counting multiples of the same object). The surviving objects included the titanium propulsion module, four steel reaction wheel assemblies, a beryllium TES gimbal, and the beryllium

Project Reviews

Reentry Survivability Analysis of the Earth Observing System (EOS)-Aura Spacecraft, Cont'd

optical bench, M 6, and scan mirror assemblies of the HIRDLS instrument. Titanium, steel, and beryllium tend to have higher survival tendencies due to the high melting temperatures of these material types (1943 K, 1644 K, and 1557 K, respectively). A component is considered demised once the total heat absorbed has reached the heat of ablation of the object. With such high melting temperatures, the heat of ablation for those six objects was never reached in the ORSAT analysis, resulting in their survival. Figure 1 shows a plot of altitude vs. downrange for the objects analyzed. A footprint length of 280 kilometers was calculated based on results from ORSAT. The total debris casualty area for all surviving objects totaled 10.49 m^2, corresponding to a total casualty risk of 1:10,540. ❖
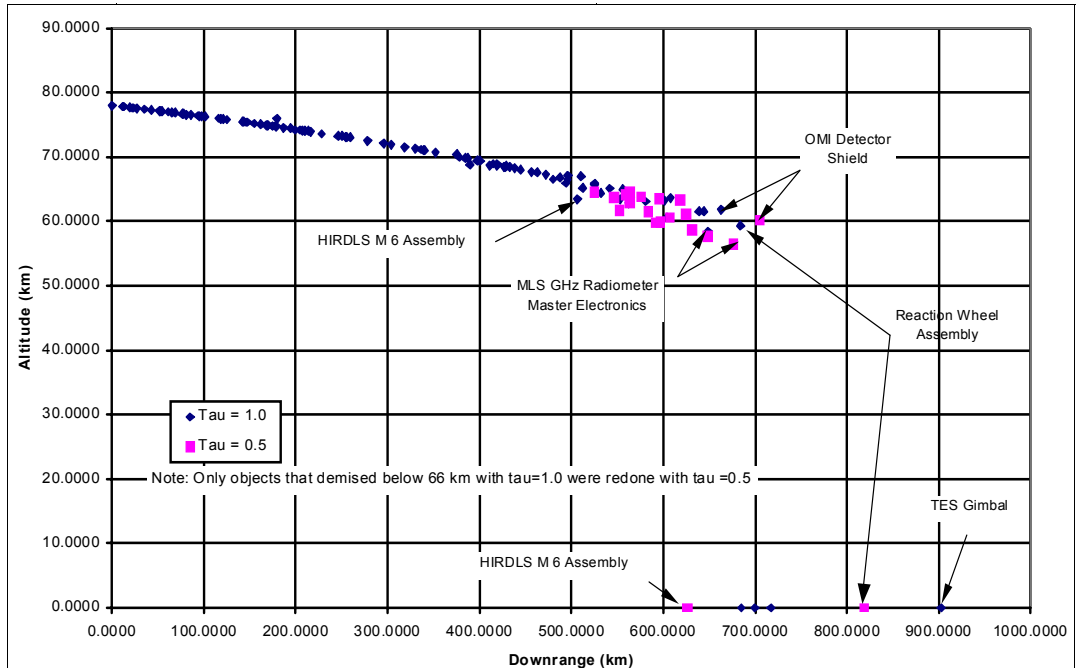

Figure 2. EOS-Aura demise altitude vs. downrange for all objects.

Meeting Report

52nd International Astronautical Congress
1-5 October 2001   Toulouse, France

The latest annual International Astronautical Congress (IAC), held in Toulouse, France, during 1-5 October 2001, once again featured a wide variety of papers on orbital debris topics. The 34th Safety, Rescue, and Quality Symposium served as the focal point for orbital debris presentations and discussions. In all, 21 papers were presented during three sessions, and three additional works were available as printed papers or viewgraphs. In all, five papers by NASA and Lockheed Martin personnel representing the NASA Orbital Debris Program Office at the Johnson Space Center were delivered (see Orbital Debris Quarterly News, Vol. 6, No. 4).

The latest world-wide orbital debris measurement and modeling efforts are bringing the international community closer to a consensus on the state of the current orbital debris environment. European researchers reported better agreement between measurements and modeling when using the new NASA breakup model first presented at the 33rd Scientific Assembly of COSPAR in July 2000. Orbital debris mitigation measures and standards stood out as a principal focus of the symposium. Design and operational practices to limit the growth of the orbital debris population are widely acknowledged as the most important near-term considerations.

The subject of orbital debris also arose during one of the several sessions of the Congress sponsored by the International Institute of Space Law. E. Jason Steptoe of the office of the NASA General Counsel presented a paper entitled "Legal Standards for Orbital Debris Mitigation: A Way Forward". Dr. Lubos Perek of the Czech Astronomical Institute offered his opinions on the "Definition of Space Debris".

The 52nd IAC also offered a convenient venue for meetings of the Inter-Agency Space Debris Coordination Committee (IADC) Steering Group and of Commission V of the International Academy of Astronautics (IAA), which has recently undertaken a study of spacecraft and launch vehicle debris mitigation options. One of the primary current activities of the IADC is the development of a set of consensus orbital debris mitigation guidelines, which are planned for presentation to the Scientific and Technical Subcommittee of the United Nations' Committee on the Peaceful Uses of Outer Space in February 2003. As a result of the recent reorganization of the IAA, Commission V will continue the work of the previous Subcommittee on Space Debris. ❖

INTERNATIONAL SPACE MISSIONS
October– December 2001

International Designator	Payloads	Country/ Organization	Perigee (KM)	Apogee (KM)	Inclination (DEG)	Earth Orbital Rocket Bodies	Other Cataloged Debris
2001-041A	PROGRESS DC-1	RUSSIA	329	335	51.6	1	0
2001-042A	ATLANTIC BIRD 2	EUTELSAT	35772	35801	0.0	1	0
2001-043A	STARSHINE 3	USA	447	454	67.0	1	0
2001-043B	PICOSAT 9	USA	793	795	67.0		
2001-043C	PCSAT	USA	793	800	67.0		
2001-043D	SAPPHIRE	USA	792	798	67.0		
2001-044A	USA 161	USA	NO ELEM. AVAILABLE			1	0
2001-045A	RADUGA 1-6	RUSSIA	35774	35803	1.3	2	5
2001-046A	USA 162	USA	NO ELEM. AVAILABLE			1	0
2001-047A	QUICKBIRD 2	USA	444	446	97.2	1	0
2001-048A	SOYUZ-TM 33	RUSSIA	381	385	51.6	1	0
2001-049A	TES	INDIA	558	565	97.7	1*	1
2001-049B	PROBA 1	ESA	551	675	97.9		
2001-049C	BIRD 2	GERMANY	547	576	97.8		
2001-050A	MOLNIYA 3-52	RUSSIA	626	39719	62.9	2	1
2001-051A	PROGRESS M1-7	RUSSIA	381	385	51.6	1	0
2001-052A	DIRECTV 4S	USA	35785	35788	0.0	1	0
2001-053A	COSMOS 2380	RUSSIA	19115	19145	64.8	2	3
2001-053B	COSMOS 2381	RUSSIA	19069	19191	64.8		
2001-053C	COSMOS 2382	RUSSIA	19114	19146	64.8		
2001-054A	STS-108	USA	353	377	51.6	0	0
2001-054B	STARSHINE II	USA	355	382	51.6		
2001-055A	JASON	USA	1334	1347	66.4	1	1
2001-055B	TIMED	USA	627	628	74.1		
2001-056A	METEOR-3M	RUSSIA	996	1016	99.6	1	1
2001-056B	KOMPASS	RUSSIA	987	1014	99.6		
2001-056C	BADR-B	PAKISTAN	986	1014	99.6		
2001-056D	MAROC-TUBSAT	GERMANY	985	1014	99.6		
2001-056E	REFLECTOR	RUSSIA	986	1014	99.6		
2001-057A	COSMOS 2383	RUSSIA	405	417	65.0	1	0
2001-058A	COSMOS 2384	RUSSIA	1415	1433	82.5	1	0
2001-058B	COSMOS 2385	RUSSIA	1417	1426	82.5		
2001-058C	COSMOS 2386	RUSSIA	1415	1419	82.5		
2001-058D	GONETS D7	RUSSIA	1412	1418	82.5		
2001-058E	GONETS D8	RUSSIA	1404	1418	82.5		
2001-058F	GONETS D9	RUSSIA	1404	1418	82.5		

* Rocket Body breakup into more than 330 pieces on 19 December.

The Johnson Space Center Orbital Debris Group

ORBITAL BOX SCORE
(as of 9 January 2002, as catalogued by US SPACE COMMAND)

Country/ Organization	Payloads	Rocket Bodies & Debris	Total
CHINA	32	310	342
CIS	1340	2529	3869
ESA	31	288	319
INDIA	21	7	28
JAPAN	68	47	115
US	957	2825	3782
OTHER	317	27	344
TOTAL	2766	6033	8799

Correspondence concerning the ODQN can be sent to:

Sara A. Portman
Managing Editor
NASA Johnson Space Center
Orbital Debris Program Office
Mail Code C104
Houston, Texas 77058

sara.a.portman1@jsc.nasa.gov

Upcoming Meetings

23-25 April 2002: Space Control Conference, Lexington , Massachusetts. The conference addresses a broad range of topics related to Space Control, including, but not limited to, Space Control Issues such as protection, simulation & modeling, and situational awareness; Space Surveillance Technology, both space and ground based; and Monitoring and Identification including object identification and status monitoring and satellite imaging.

25 February – 8 March 2002: 39th session of the Scientific and Technical Subcommittee (STSC) of the United Nations' Committee on the Peaceful Uses of Outer Space COPUOS), Vienna, Austria. The annual meeting of the STSC will once again include space debris on its agenda. The special topic for this session is space debris impact hazards and shielding. National delegations will address this subject as well as other space debris-related issues and efforts. The Inter-Agency Space Debris Coordination Committee (IADC) will also present a summary of its recent activities, including a status on its development of a set of consensus space debris mitigation guidelines. These guidelines and existing national guidelines will be the primary space debris focus during the 40th session of the STSC in 2003.